Critical Onset of Layering in Sedimenting Suspensions of Nanoparticles

A. V. Butenko,[1] P. M. Nanikashvili,[2] D. Zitoun,[2] and E. Sloutskin[1*]
[1]Physics Department and Institute for Nanotechnology and Advanced Materials, Bar-Ilan University, Ramat-Gan 52900, Israel
[2]Chemistry Department and Institute for Nanotechnology and Advanced Materials, Bar-Ilan University, Ramat-Gan 52900, Israel
(Received 3 September 2013; published 7 May 2014)

We quantitatively study the critical onset of layering in suspensions of nanoparticles in a solvent, where an initially homogeneous suspension, subject to an effective gravity a in a centrifuge, spontaneously forms well-defined layers of constant particle density, so that the density changes in a staircaselike manner along the axis of gravity. This phenomenon is well known; yet, it has never been quantitatively studied under reproducible conditions: therefore, its physical mechanism remained controversial and the role of thermal diffusion in this phenomenon was never explored. We demonstrate that the number of layers forming in the sample exhibits a critical scaling as a function of a; a critical dependence on sample height and transverse temperature gradient is established as well. We reproduce our experiments by theoretical calculations, which attribute the layering to a diffusion-limited convective instability, fully elucidating the physical mechanism of layering.

DOI: 10.1103/PhysRevLett.112.188301 PACS numbers: 47.57.ef, 47.55.pb, 82.70.Kj

Sedimentation of micro- and nano-particles in a solvent under gravity is common in bio- and nano-technology [1], occurring in a wide range of geophysical systems [2] and limiting the shelf life of food products and pharmaceuticals [3]. Sedimentation is also widely used as an analytical tool for industrial, medical [4], and research applications [5–7]. Under most common experimental conditions, the density of particles in a sedimenting fluid suspension is a continuous function of time and spatial coordinates [8]. However, occasionally, the density of particles develops multiple (roughly) equispaced plateaus, thus adopting a staircaselike appearance along the axis of sedimentation. This phenomenon, called "layering" or "stratification," has been known for more than a century [9–11]. Yet, most previous experimental realizations of this effect employed micron-sized particles [10,12,13], for which the layer structure is highly sensitive to tiny temperature gradients [10,12,14], prohibiting extraction of quantitative experimental information. Other experiments employed particles with high or unknown polydispersity [6,9], which limited the availability of interpretable experimental data. As a result, the physical mechanism of layering in sedimenting suspensions remained ambiguous [15], with several competing theoretical scenarios attributing the layering to either Burger's shock formation [16], spinodal decomposition [12], vertical streaming flows [2], spontaneous formation of magic number clusters [6,14,17], long-range hydrodynamic interactions [18,19], or convective instability [10,20]. Quantitative experimental information, which would allow the true mechanism of layering to be unequivocally identified, was missing.

We follow the full dynamics of layer formation in sedimenting suspensions of several different types of nanoparticles in various organic solvents subjected to an effective gravity in a centrifuge, employing light transmission (LT) through the samples. We demonstrate that by using nanoparticles, the layering phenomena are much more robust than in the previous studies [10,20]; this system allows quantitative and reproducible measurements to be collected with our experimental setup. Furthermore, this setup allows the effective gravity a, measured in the units of $g = 9.8\ \mathrm{m/s^2}$, to be varied; we use it to study the critical onset of the layering effect, where pattern formation by layering overcomes the significant thermal diffusion of the nanoparticles. We demonstrate that in this regime, the number of layers N in a sample exhibits a unique power-law scaling as a function of a and the height H of initial suspensions; the dependence on H of the critical effective gravity a_c, below which the layers do not form, is explored as well. We reproduce most of our observations by numerical calculations, employing a hydrodynamical model that attributes the layering to a convective instability [10,20]. We suggest that the spontaneous layering in suspensions of nanoparticles may serve as a basis for future analytical techniques for nanoscale colloids, and may have important applications in self-assembly of metamaterials.

We prepare Cu@Ag and pure Ag nanoparticles, stabilized by either an oleylamine or a dodecanethiol surface monolayer [21], and suspend them in pure hexane or heptane at a low volume fraction $c_0 = 10^{-4} - 10^{-3}$; these particles form promising inks for inkjet printing [21]. The average diameter σ and size distributions $P(\sigma)$ of the particles are measured by transmission electron microscopy (TEM). Most samples exhibit a simple Gaussian $P(\sigma)$, peaking between 10 and 20 nm, with a width of ~4 nm (see Supplemental Material [22]). We load the initially homogeneous fluid suspension into an analytical tabletop centrifuge (Lumifuge), where a is in the range $200 < a < 2500$.

Our centrifuge measures LT profiles $I(x)$ through the suspension in real time during the centrifugation, as shown in Fig. 1. The cooling element of our setup, positioned at the bottom, sets the direction of the temperature gradient $\hat{z}$ [23], so that the temperature drop over the sample is $\tilde{\Delta} \approx 0.4$ K [22]. We fill our suspensions into polyamide cuvettes to a height $5 < H < 35$ mm; the cuvettes are then loaded horizontally into the centrifuge.

The suspension is initially homogeneous and opaque for LT. Sedimentation of particles by effective gravity forms a particle-free supernatant region in the sample (on the left hand side of Fig. 1); LT through this region is $>95\%$. For silica colloids [24,25] in ethanol, the supernatant is separated from the sedimenting suspension by a relatively sharp interface, or sedimentation front, which propagates along the effective gravity at a constant speed $\mathbf{v_0}$, for which the centrifugal force is balanced by the Stokes drag [7], see Fig. 2(a). With nanoparticles, the sedimentation front gets increasingly smeared at short times due to their significant polydispersity [green dotted curve in Fig. 2(b)]. Strikingly, a staircaselike variation of transmission is then developed [Fig. 2(b)], indicating formation of distinct layers of constant density [10,12,13]. This effect cannot be attributed to particle size or shape segregation [9], as $P(\sigma)$ of our particles is single peaked (Fig. S9) and the particles appear rounded by TEM [22]. Similarly, particle clustering [6,14,17] is excluded, as it does not produce uniform steps in LT; also, sedimentation velocities of compact n-particle clusters scale as $n^{2/3}$ [26], while the experimental velocities of plateau boundaries are all very close together [10,12]. Varying the interparticle potentials by changing the particles' surface layer from oleylamine to dodecanethiol, or replacing hexane with heptane, does not significantly alter the appearance of layers; increasing particle density makes the layering vanish. Both of these observations rule out the aggregation scenario.

More recent studies [10,20] suggest that the layering is driven by a convective instability. In particular, a tiny thermal gradient normal to the sedimentation axis was conjectured [10] so that the two sides of the sample are at a temperature difference $\tilde{\Delta}$; this increases the average gravimetric density of the suspension on one side of the cuvette by $\delta\rho$, resulting in an increased sedimentation rate on that side [inset to Fig. 3(a)]. For a homogeneous sample, an individual convection roll should form, spanning the whole sample. However, when the initial particle density $c(x)$ is sloped, the average gravimetric density of the suspension (with the particles included) $\rho(x)$ is sloped as well. As a result, the densities on both the cold and the hot sides of the cuvette will match again [20] if the sides are mutually shifted by a distance $\Lambda = \delta\rho(d\rho/dx)^{-1}$ along $\mathbf{g}$. This sets the width of the layers to be roughly equal to Λ; a more accurate estimate requires the full details of roll formation dynamics to be taken into account [20]. Once the convection rolls form, the particle density within each roll is homogenized and levels of equal density flatten out, giving rise to a staircaselike appearance of transmission profiles, such as in Fig. 2(b). According to this model, the layering phenomenon is an example of a spontaneous symmetry breaking, akin to the Belousov-Zhabotinsky patterns in chemistry or the Liesegang layers in geology [11,27]. Since even very small $\tilde{\Delta}$ may be sufficient for the layering to occur, a direct measurement of $\tilde{\Delta}$ inside the centrifuge is challenging; yet, as in previous works [10], we could almost completely eliminate the layering by thermal shielding of the samples, which were wrapped for that purpose with a copper foil (see Fig. S1 [22]). More interestingly, the layering phenomenon is notoriously sensitive to the shape of $P(\sigma)$. We could selectively eliminate the layering in a part of the suspension by truncating the low-σ wing of particle size distribution [22]. Remarkably, the asymmetry of $P(\sigma)$ is difficult to measure in nanoparticles by either classical light scattering [28,29] or modern analytical centrifugation

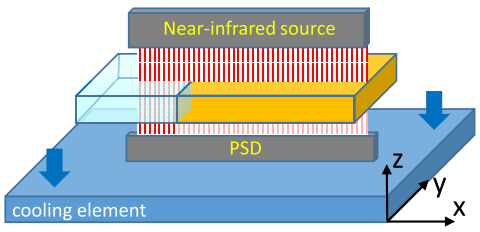

FIG. 1 (color online). Experimental setup. An optically transparent cuvette ($2 \times 8 \times 50$ mm), loaded with the suspension (orange) is centrifuged in the xy plane; the centrifugal acceleration is $\mathbf{a} \equiv a\hat{x}$. The sample is illuminated with a planar sheet of light at 870 nm (vertical red lines). LT profiles are measured with a position sensitive detector (PSD). Thick down-oriented arrows indicate the heat flow direction.

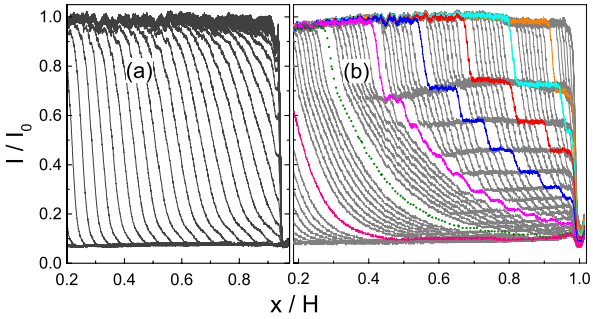

FIG. 2 (color online). LT profiles along the sedimenting suspensions, obtained for a suspension of (a) silica colloids ($\sigma \approx 0.5$ μm) and (b) Cu@Ag nanoparticles. Profiles corresponding to different time points after the beginning of the centrifugation are overlayed such that the time separation between subsequent curves is 30 sec in (a) and 112 sec in (b); $H = 29$ mm. While the profiles in (a) are monotonic, they adopt a steplike shape in (b) at long centrifugation times, indicating the onset of layering. A solid sediment is formed for $x/H > 0.95$, blocking the LT in this region. The same data are shown animated in the Supplemental Material [22].

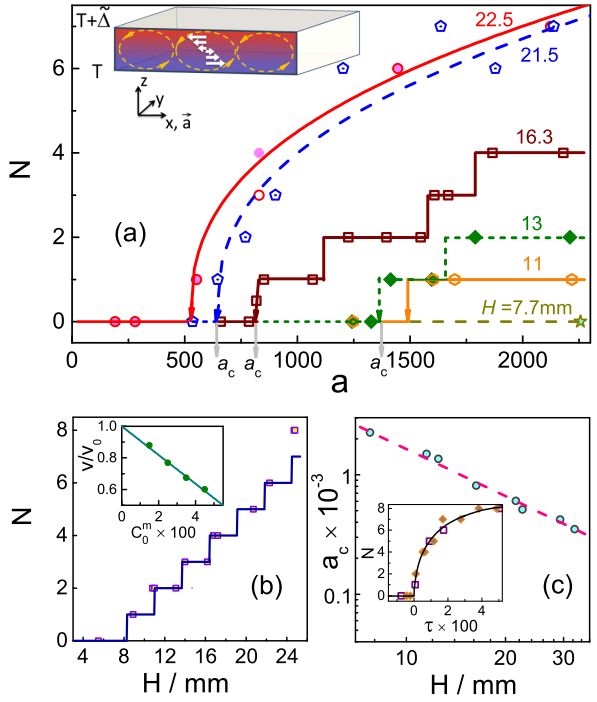

FIG. 3 (color online). (a) The experimental number of layers N observed in samples of different initial height H (see labels) varies as a function of the effective gravity a; no layering is observed for $a < a_c$. Inset: Transverse temperature gradient induces a sedimentation velocity difference between sample edges. Velocities, in the frame comoving with the center of mass of the suspension, are represented by white arrows; color map represents the temperature. (b) For a constant $a = 1.6 \times 10^3$, N increases with H; no layering occurs for $H < H_c = 8$ mm. Inset: The sedimentation front velocities of Ag nanoparticles at short centrifugation times, as a function of the particle mass fraction $C_0^m \approx 15C_0$, normalized by the sedimentation velocity of a free particle v_0. (c) The critical threshold for layering scales as $a_c \propto H^{-4/3}$; the fitted exponent accuracy is ± 0.06. Inset: Experimental (open squares) and theoretical (solid rhombii) N coincide, plotted as a function of dimensionless offset τ of the temperature gradient.

methods [5], while TEM can only be carried out with dried particles. Therefore, the unique sensitivity of layering to this asymmetry suggests that new analytical techniques exploiting the layering patterns at preset temperature gradients may be developed, which would allow full characterization of $P(\sigma)$ in fluids.

As a more direct and quantitative test of the convective instability model, we exploit the high reproducibility of the layering transition and the variability of sedimentation velocity in a centrifuge to study the critical conditions for the onset of layering; such a test was impossible in earlier experiments, where even the radiated body heat of the experimenter was sufficient to destroy the layer pattern [10,12], making it very challenging to collect quantitative experimental results. As the simplest quantitative measure of layering, we count the number of layers N appearing in the sample of initial height H. Strikingly, the number of layers exhibits a critical scaling $N \propto |a - a_c|^{0.39\pm0.05}$, as shown in Fig. 3(a); the overlapping open red and solid magenta circles [Fig. 3(a)], obtained for different samples, demonstrate good reproducibility. N is directly proportional to H, except for the fine staircaselike structure due to the integer nature of N [see Fig. 3(b)]; this indicates that the critical thickness of an individual layer, before the next layer starts forming, is independent of the sample size. For $H < H_c$, the distance passed by the sedimentation front is small, so its broadening is negligible and the resulting particle concentration gradient dc/dx is too steep for the layering to occur [22]. More surprising is the $a_c(H)$ scaling [Fig. 3(c)]; as the maximal broadening of the sedimentation front for a given H does not depend on a, we carry out a full numerical solution of a system of partial differential equations (PDEs) describing the convective instability [10,20], in an attempt to account for the observed scaling.

For nanoparticles in a solvent, the Reynolds numbers are small, and the equations of motion for an incompressible fluid in Stokes approximation are $\nabla p = \rho(\nu \triangle \mathbf{u} + g\mathbf{a})$ and $\nabla \cdot \mathbf{u} = 0$, where $\mathbf{u}$ is the convection velocity and p is the pressure [20,30]; here the suspension is treated as an effective medium of kinematic viscosity ν. For the particles, the mass conservation is [20] $\dot{c} + \mathbf{u} \cdot \nabla c + \mathbf{v_0} \cdot \nabla c = D \triangle c$, where the hindrance of dynamics by particle crowding [31] was neglected in our range of c and D is the diffusion coefficient of the nanoparticles. Retaining the c and T dependence in the forcing term [20], we obtain (to the leading order) from the equation of motion $\nabla p = \rho\nu \triangle \mathbf{u} + \Delta\rho c g\mathbf{a} - (2d)^{-1} z\beta\rho\tilde{\Delta} g\mathbf{a}$, where $\beta \approx 10^{-3}$ °C^{-1} is the coefficient of thermal expansion and $2d = 2$ mm is the thickness of our cuvettes (Fig. 1). To reduce the problem to one spatial dimension, an approximate solution along z conforming with the geometry of roll formation is guessed [20]; this is known as the Galerkin method. The dimensionless version of the resulting PDE [22] includes only four parameters: $\alpha \equiv |\mathbf{v_0}|/U$, $\gamma \equiv \sigma/2d$, $\delta \equiv D/|\mathbf{v_0}|d$, and c_0, where $U \equiv \beta\tilde{\Delta} g a d^2/\nu$ sets the scale of convection velocities, $|\mathbf{v_0}| = \Delta\rho\sigma^2 g a/18\nu\rho_0$, and $\Delta\rho$ is the excess gravimetric density of the particles, compared to that of the solvent ρ_0; the dimensionless time is $t_r \equiv t|\mathbf{v_0}|/d$. We solve the equations for $\tilde{\Delta} = 0.1$ K, employing the finite difference method, with hard boundary conditions set at the high-x end of the cuvette. For the layering to occur, we use a linearly sloping $c(x) = c_0[1 + p(x - H/2)]$ for the initial conditions, where we choose $p = 0.16$ cm^{-1}; this is comparable to the experimental $c(x)$, which is significantly broadened due to particle polydispersity prior to the onset of layering [Fig. 2(b)]. The PDE exhibit formation of density layers; the layers move along the effective gravity and disappear as they reach the bottom of the sample, where a dense sediment forms [22]. The total number of layers forming in a sample N scales as $N \propto |a - a_c|^{0.30\pm0.01}$ [Fig. 4(a)], in good agreement with the experiment, which validates the theoretical model. To collapse together data obtained for

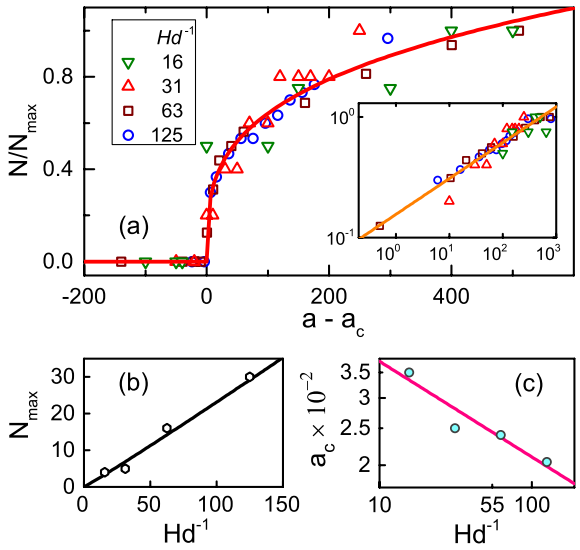

FIG. 4 (color online). (a) The theoretical number of layers N in samples of different height H (see legend) exhibits a critical behavior as a function of the effective gravity a. Inset: Same data on a log-log scale. N is scaled by $N_{\max}$ to make all data collapse together; $N_{\max}$ values are shown in (b). (c) The scaling of the critical threshold for layering $a_c \propto H^{-0.24\pm0.06}$ is less steep than in experiment [see Fig. 3(c)]. Our PDE are stiff and numerical divergences occur when the layers become exceedingly sharp; to avoid this numerical instability, we set $d = 0.2$ mm [22].

different values of H, we scale each $N(a)$ curve by an arbitrary $N_{\max}$, as shown in Fig. 4(a). These $N_{\max}$ values are linear in H, see Fig. 4(b), much like in the experiment [Fig. 3(b)]. According to our theoretical model, the critical sample size for layering is $H = 0$; this is reasonable, as a finite distance H_c is required in the experiment for the sedimentation front propagation to develop the linear $c(x)$ profile, used as the initial condition for our PDE. Thus, overall, the agreement of this model with the experiment is very good; the only exception is the theoretical $a_c(H)$ scaling [Fig. 4(c)], which is quantitatively different from the experimental one; this suggests that a more elaborate theoretical model, possibly taking into account the spread of experimental sedimentation velocities due to polydispersity, both before and after the onset of layering, may be needed to reproduce the experimental observations in full detail.

The good agreement of these PDE with the experiment allows the role of thermal diffusion in this system to be investigated. The calculated average layer width $\lambda^\star \equiv \lambda(t^\star)$ at the onset of layering $t = t^\star$ exhibits a diffusive scaling $\lambda^\star \sim \sqrt{Dt^\star}$ [22], suggesting that $t^\star$ may be determined by a competition between convection and diffusion. For a given time t, structural details finer than $\sqrt{Dt}$ are smeared by diffusion, while the typical length scale for structure formation by the convection rolls is proportional to Ut. At $t = t^\star$ both effects are balanced, so that $t^\star = DU^{-2}$. In our PDE, D and a appear only through the ratio D/a, which leads us to assume that the scaling of the dimensionless $t^\star$ is $t_r^\star \sim (D/a)^\mu$. In such case, $t^\star \sim a^{-1}(D/a)^\mu$, which is indeed obtained in Figs. S8 (b),(c) for $\mu \approx -0.3$ [22]. Combined with the above, we obtain $\lambda^\star \sim (D/a)^{(\mu+1)/2} \sim (D/a)^{0.35}$, so that $N \sim 1/\lambda^\star \sim (a/D)^{0.35}$; this is in perfect agreement with the experiment [Fig. 3(a)] and emphasizes the role of D, which is much higher in our nanoparticles compared to emulsions employed in earlier work [10]. Finally, we systematically vary N by tuning of $\tilde{\Delta}$; for this purpose, we introduce a static electrically heated copper plate above the sample, controlling the temperature offset $\tilde{\Delta}_{\exp}$ between this plate and the cooling element (Fig. 1). The results are shown together with the theoretical N in the inset to Fig. 3(c), where $\tau \equiv (\tilde{\Delta} - \tilde{\Delta}_c)/(\tilde{\Delta}_c + B)$; $\tilde{\Delta}_c$ is the value of $\tilde{\Delta}$ at the onset of layering, and $B = 0$ for the theoretical data. To account for the difference between $\tilde{\Delta}_{\exp}$ and $\tilde{\Delta}$, we fit $B = 120$ K as a free parameter for the experimental data, replacing $\tilde{\Delta} \to \tilde{\Delta}_{\exp}$ and $\tilde{\Delta}_c \to \tilde{\Delta}_{c,\exp} \approx 0.9$ in the expression for τ. The perfect agreement thus obtained for $N(\tau)$, which necessitated a full solution of the PDEs and could not be guessed from the above-mentioned simplistic scaling of Λ, is a strong support for our theoretical model. Though in other sedimentation instabilities, driven by hydrodynamic interactions, finite wave number structures form for $D > 0$ [18,19], the observed $\tilde{\Delta}$ dependence is unique; future experiments should allow λ to be measured at the steady state conditions ($t \gg t^\star$) and compared with the predictions of our model and other theoretical scalings [18,19].

The formation of convection rolls, demonstrated to be the physical mechanism of layering, modifies the sedimentation hydrodynamics. In particular, the sedimentation velocity, which is supposed to follow the classical $v(c) = v_0(1 - 6.55c_0)$ Batchelor's law [26] at $c_0 \ll 1$, is modified in our case even for $t \ll t^\star$; see inset to Fig. 3(b), where the slope $|dv(c)/dc|$ exceeds the Batchelor's law prediction by a factor of $\sim$20. Other hydrodynamic instability has recently been demonstrated to *increase* the absolute value of $v(c)$ for macroscopic spheres under confinement [32]. These observations call for more advanced theoretical models to describe the early stages of sedimentation.

In conclusion, we have employed suspensions of nanoparticles to obtain a reproducible and controllable layering, and have followed the critical scaling laws and compared them with theory, demonstrating a semiquantitative agreement; this proves that the formation of layers is driven by a convective instability, which competes with thermal diffusion. Other mechanisms, suggested in earlier works, are incompatible with our observations. Finally, the achieved understanding of the basic physics of layering, and also the observed reproducibility of this effect with nanoparticles, open a broad perspective for future research exploring similar phenomena in the presence of particle crowding, in non-Newtonian solvents, in complex temperature fields, and in cuvettes of nontrivial geometry; a wide range of

objectives can thus be pursued, from the basic science of fluid and solid [7] sediments to the development of analytical methods for nanoparticle characterization and nanopatterning technologies.

We are grateful to T. Sobisch, M. Shmilovitz, N. Shnerb, D. A. Kessler, and S. Shatz for insightful discussions. The authors thank A. Muzikansky for synthesis of early Cu@Ag samples and D. Fridman for technical assistance. This research is supported by the Israel Science Foundation (Grants No. 85/10 and No. 1668/10). P. M. N. acknowledges Ministry of Absorption for funding.

*eli.sloutskin@biu.ac.il

[1] E. C. Cho, Q. Zhang, and Y. Xia, Nat. Nanotechnol. **6**, 385 (2011).
[2] W. H. Bradley, Science **150**, 1423 (1965).
[3] S. Calligaris and L. Manzocco, in *Shelf Life Assessment of Food*, edited by M. C. Nicoli (CRC Press, Boca Raton, USA, 2012).
[4] H. L. Haber, J. A. Leavy, P. D. Kessler, M. L. Kukin, S. S. Gottlieb, and M. Packer, N. Engl. J. Med. **324**, 353 (1991).
[5] R. P. Carney, J. Y. Kim, H. Qian, R. Jin, H. Mehenni, F. Stellacci, and O. M. Bakr, Nat. Commun. **2**, 335 (2011).
[6] J. Boom, W. S. Bont, H. P. Hofs, and M. De Vries, Molecular biology reports **3**, 81 (1976).
[7] S. R. Liber, S. Borohovich, A. V. Butenko, A. B. Schofield, and E. Sloutskin, Proc. Natl. Acad. Sci. U.S.A. **110**, 5769 (2013).
[8] K. Benes, P. Tong, and B. J. Ackerson, Phys. Rev. E **76**, 056302 (2007).
[9] W. H. Brewer, Clays Clay Miner. **13**, 395 (1884).
[10] D. M. Mueth, J. C. Crocker, S. E. Esipov, and D. G. Grier, Phys. Rev. Lett. **77**, 578 (1996).
[11] T. Shinbrot and F. J. Muzzio, Nature (London) **410**, 251 (2001).
[12] D. Siano, J. Colloid Interface Sci. **68**, 111 (1979).
[13] N. B. Uriev and I. I. Bardyshev, Colloids Surf. A **225**, 25 (2003).
[14] W. S. Bont, H. P. Hofs, and M. De Vries, Colloid Polym. Sci. **257**, 656 (1979).
[15] R. Piazza, S. Buzzaccaro, and E. Secchi, J. Phys. Condens. Matter **24**, 284109 (2012).
[16] W. van Saarloos and D. A. Huse, Europhys. Lett. **11**, 107, (1990).
[17] W. S. Bont, Mol. Biol. Rep. **36**, 959 (2009).
[18] D. Saintillan, E. S. G. Shaqfeh, and E. Darve, Phys. Fluids **18**, 121503 (2006).
[19] É. Guazzelli and J. Hinch, Annu. Rev. Fluid Mech. **43**, 97 (2011).
[20] A. E. Hosoi and T. F. Dupont, J. Fluid Mech. **328**, 297 (1996).
[21] A. Muzikansky, P. Nanikashvili, J. Grinblat and D. Zitoun, J. Phys. Chem. C **117**, 3093 (2013).
[22] See Supplemental Material at http://link.aps.org/supplemental/10.1103/PhysRevLett.112.188301 for dependence of layering on $\tilde{\Delta}$, d, and particle polydispersity; details on PDE solution, scaling laws, and dynamics are discussed and animated.
[23] T. Sobisch, Lumifuge (private communication).
[24] W. Stöber, A. Fink, and E. Bohn, J. Colloid Interface Sci. **26**, 62 (1968).
[25] N. M. Abrams and R. E. Schaak, J. Chem. Educ. **82**, 450 (2005).
[26] R. J. Hunter, *Foundations of Colloid Science*, (Oxford University Press, New York, 2009), 2nd ed.
[27] S. Thomas, I. Lagzi, F. Molnár, and Z. Rácz, Phys. Rev. Lett. **110**, 078303 (2013).
[28] B. J. Frisken, Appl. Opt. **40**, 4087 (2001).
[29] P. N. Pusey and W. van Megen, J. Chem. Phys. **80**,3513 (1984).
[30] L. D. Landau and E. M. Lifshitz, *Fluid Mechanics* (Pergamon, New York, 1987), 2nd ed.
[31] G. K. Batchelor, J. Fluid Mech. **52**, 245 (1972).
[32] S. Heitkam, Y. Yoshitake, F. Toquet, D. Langevin, and A. Salonen, Phys. Rev. Lett. **110**, 178302 (2013).